Childs Nerv Syst (2006) 22:1451–1456
DOI 10.1007/s00381-006-0118-3

ORIGINAL PAPER

Chiari I anatomy after ventriculoperitoneal shunting: posterior fossa volumetric evaluation with MRI

Ferdnand C. Osuagwu · Jorge A. Lazareff · Shayan Rahman · Suzie Bash

Received: 18 January 2006 / Published online: 30 May 2006

Abstract
Introduction Cephalocranial disproportion was said to be responsible for Chiari I malformation after ventriculoperitoneal shunt. We aimed to evaluate if the volumetric characteristics of Chiari I after a ventriculoperitoneal shunt was due to a general volumetric reduction and if it is restricted to the posterior fossa.
Results Our results show that the posterior fossa volume, cisternal, clival length, and posterior cranial fossa volume ratio were reduced in the shunted group compared to the controls ($p<0.05$). Cerebellar and supratentorial volumes were similar between both groups. Craniocaudal extent, inferior, and superior tonsillar herniations were greater in the shunted group than control ($p<0.05$). The frontal occipital horn ratio in both groups was within normal range.
Discussion Chiari I anatomy after a ventriculoperitoneal shunt could develop in children and we propose a "posterior cranial fossa disproportion" rather than a "cephalocranial disproportion."

Keywords Acquired Chiari · Posterior cranial fossa reduction · Hydrocephalus · Intraventricular hemorrhage · V-P shunt

F. C. Osuagwu
Department of Anatomy, University of Ibadan, Ibadan, Nigeria

F. C. Osuagwu · J. A. Lazareff (✉) · S. Rahman
Division of Neurosurgery, UCLA School of Medicine, Box 957039, Los Angeles, CA 90095-7039, USA
e-mail: jlazareff@mednet.ucla.edu

S. Bash
Department of Radiology, UCLA School of Medicine, Box 957039, Los Angeles, CA 90095-7039, USA

Introduction

In the past years, we have observed that some children who had a ventriculoperitoneal shunt (VP shunt) for neonatal hydrocephalus later present with symptoms suggestive of Chiari I.

The symptoms would come and wane, or be persistent but not severe. In the cases in which the clinical development demanded a brain MRI, we found radiographic evidence of a crammed posterior cranial fossa with or without descent of the cerebellar tonsils. None of the patients had preoperative radiographic evidence of Chiari malformation.

This phenomenon of brain tissue constrained within the skull in shunted children was described by Hoffman and Tucker in 1976 [1]. They labeled it as "cephalocranial disproportion" due to shunting in patients with hydrocephalus.

To determine if there is such a volumetric disproportion between brain and skull, we conducted this study in nine children who presented with Chiari-like symptoms after VP shunt and compared our findings with a similar cohort of non-shunted age matched controls.

Materials and methods

Patients and control subjects

Children who presented with symptoms of Chiari I malformation years after a perinatal VP shunt on account of hydrocephalus secondary to intraventricular hemorrhage were included in the study if there was a pre-shunt CT or MRI and a post-shunt MRI.

Patients were excluded from the study if the pre-shunting CT demonstrated any evidence of posterior fossa crowding, with specific attention to the anatomy of the craniovertebral

Table 1 Quantitative measurements of the parameters measured in the posterior cranial fossa of both shunted and control groups

Variable	Control group (n=8)	Shunted group (n=9)	p value
Age (years)	6.5±1.7	7.3±1.3	0.7
Gender (m/f)	2m/6f	3m/6f	
Linear measurements (mm)			
Clivus	33.1±1.3	26.4±2.3	0.02
Length of cerebellum	59.1±5.5	48.6±2.4	0.11
Tonsillar herniation	−2.2±1.8	8.2±1.8	0.001
Upper herniation through the incisura	0.0±0	14.6±4.6	0.013
Prepontine cistern	7.8±0.5	4.5±0.8	0.004
Premedullary cistern	9.9±0.6	6.3±0.8	0.002
Volumetric measurements (ml)			
Cerebellum	116.8±4.6	114.1±8.8	0.8
Posterior cranial fossa	167.3±5.2	137.9±8.5	0.011
Supratentorial	924±52.5	1,058.7±50.6	0.09
Ratios			
Frontal–occipital horn ratio	0.34±0.008	0.39±0.02	0.07
PFV/SV×100 (Posterior fossa volume ratio)	18.5±1.3	13.1±0.8	0.003

junction; narrowing of the perimedullary, retrocerebellar, or prepontine cisterns; abnormal size or configuration of the cerebellar tonsils; tonsillar descent below the foramen magnum; or superior cerebellar herniation through the incisura. All patients must have at least a pre-shunt CT and post-shunt MRI for inclusion in the study.

If hydrocephalus was present on the post-shunting MRI, the patient was excluded from the study. Nine study patients were identified according to the inclusion and exclusion criteria.

Eight age-matched controls were sequentially selected from the same time period, all of which had an MRI done for other medical reasons, with symptoms not referable to the posterior fossa. Control patients were excluded from the study if abnormal posterior fossa anatomy or hydrocephalus was present.

The study group was made up of three boys and six girls, ranging in age from 2 to 15 years (mean age 7.3±1.3; see Table 1) at the time of the post-shunt MRI. All patients received a VP shunt with distal slit valve (manufactured by Codman). The control group consisted of two boys and six girls who were sex-matched to their shunted group peers with age ranging from 2 to 14 years (mean age 6.5±1.7; p=0.7). The signs and symptoms that the shunted group patients presented with are shown in Table 2.

Three patients within the shunted group had posterior fossa decompression surgery done, and these patients responded well to these procedures with improvement in their clinical status.

Imaging and measurements

Pre-shunting CT images in the study group were acquired on a single (GE CTi 9800) or multidetector (GE Lightspeed 4 Detector) scanner using a slice collimation of 5 and a pitch of 1.5. Post-shunting MR images in both the control and study groups were acquired on a 1.5T Siemens Magnetom Vision or GE LX Scanner. The studies all included at least an axial T1, T2, FLAIR, and sagittal T1 sequence, but only the sagittal T1 sequence was utilized for postprocessing toward volumetric and linear measurements. Axial MRI sequences were not selected for postprocessing as the obliquity of the superior tentorial leaf and variable slice angulation at the level of the foramen magnum precluded reliable posterior fossa volumetric measurements. However, the frontal–occipital horn ratio was evaluated using the axial images. The sagittal T1 sequences were acquired using TR 400-650 ms; TE 15 ms; bandwidth 15; slice thickness 4; spacing 1; FOV 22; matrix 256×192; frequency direction, superior to inferior.

The CT images were initially postprocessed by web-fetching the data set to the Vitrea workstation (Vital Images), Versions 3.0–3.3, (Dual Processor 850 MHz–1GHz Pentium III) for 3-D reformation, but it became clear that the varied slice angulation at the level of cranioverte-

Table 2 The signs and symptoms that the patients with acquired Chiari 1 anatomy presented with

Symptoms and signs	Number of Shunted patients (n=9)
Headache	7
Vomiting	9
Nausea	6
Nystagmus	2
Strabismus	2
Hearing impairment	1
Fainting spell	1
Apnea	1

Fig. 1 Measurements of posterior cranial fossa volume (PCFV) using the T1-weighted sagittal MRI. The length of the clivus was measured from the top of the dorsum sellae (**a**) to the basion (**b**). The extent of cerebellar tonsillar herniation was measured from the tips of the cerebellar tonsils to a line drawn between the basion (**b**) and the opisthion (**c**), which represents the level of the foramen magnum. Other parameters measured include the cerebellar volume, prepontine cistern (PPC), premedullary cistern (PMC), and maximal craniocaudal extent of the cerebellum (**f**), supratentorial volume (SV)

bral junction precluded accurate, reliable measurements of the posterior fossa, so the data sets were then visually inspected by a neuroradiologist to ensure no evidence of tonsillar crowding at the craniovertebral junction.

The sagittal T1 magnetic resonance images of each subject in both the control and study groups were postprocessed by web-fetching the data set to the Vitrea workstation (Vital Images), Versions 3.7, (Dual Processor 850 MHz–1GHz Pentium III) for 3-D quantitative interactive volumetric rendering using the free-sculpting tool. The sagittal contour of the posterior fossa was manually traced on each of the 4-mm thick slices to obtain a 3-D automated surface view of the posterior fossa. Automated measurements of the surface area (centimeters^2) and

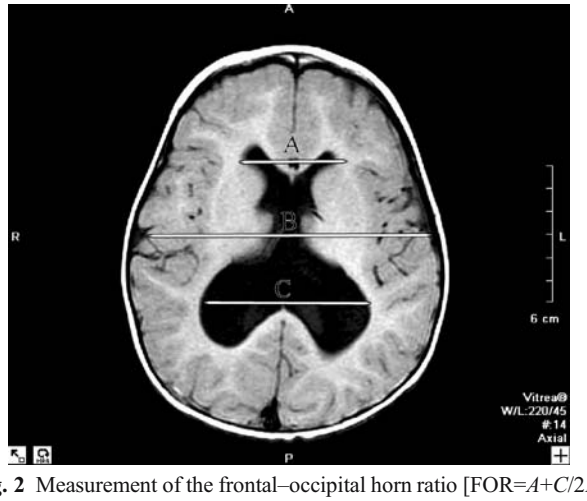

Fig. 2 Measurement of the frontal–occipital horn ratio [FOR=A+C/2B]

volume (milliliters) of the posterior fossa were then digitally rendered. The posterior fossa was defined by both osseous and dural marginal anatomy, with the posterior border of the clivus and dorsum sellae as the anterior border, the line between the basion and opisthion as the caudal border, and the anterior margin of the occipital calvarium as the posterior border. A line extending between the posterosuperior margin of the dorsum sellae to the straight sinus extending posteriorly along the superior tentorial leaf to the level of the torcula was the superior border (Fig. 1). The supratentorial region was defined as the area above the portion defined as posterior cranial fossa. This is a slight modification of the Krogness' definition [2] that the supratentorial region is the area above the Twinning's line, while the area below it is the posterior cranial fossa (infratentorial region).

Using the free-sculpting tool, the volume of the cerebellum was also obtained for each subject in both the study and control groups. The cerebellar volume measurements were not limited to cerebellar tissue located within the defined osseous and dural borders of the posterior fossa. The midline sagittal T1 slice was then utilized to quantitatively measure the anteroposterior diameter of the premedullary cistern at the level of the opisthion and prepontine cistern at the level of the sphenooccipital synchondrosis. The midline sagittal T1 slice was defined as the slice that demonstrated both the pituitary infundibulum and the aqueduct of Sylvius. Anteroposterior measurements were obtained on the 2-D sagittal view and confirmed on the correlative axial 2-D multiplanar reformatted view.

The sagittal midline T1 image was also used to measure the length of the clivusand the maximum craniocaudal length of the cerebellum [3].

The craniocaudal dimension of the cerebellar tissue, which was located beyond the superior and inferior borders of the posterior fossa, was also measured on the midline image, and this tissue was designated as the amount of superior and inferior tonsillar herniation, respectively. Inferior tonsillar herniation was defined as a vertical line measured from the lower tip of the cerebellar tonsil to the horizontal line drawn from the opisthion to the basion (level of the foramen magnum). A positive value indicates tonsillar herniation below the foramen magnum, while a negative value indicates an undescended tonsil. Similar measurements were obtained for the amount of cerebellar tissue herniating superiorly through the incisura as defined by the vertical measurement of cerebellar tissue located above the superior border of the posterior fossa.

The posterior fossa volume ratio was calculated by dividing the posterior fossa volume with the supratentorial and multiplying it by 100 [2, 4].

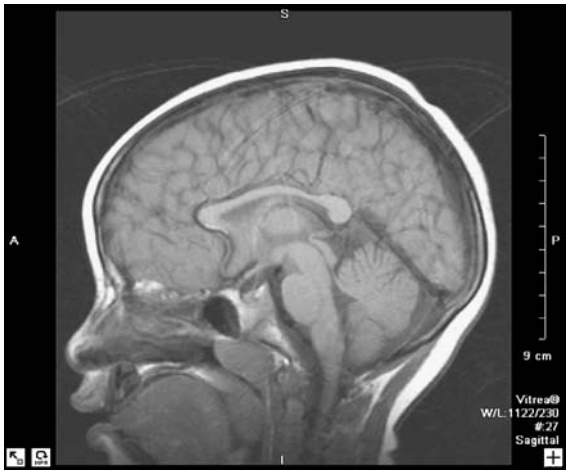

Fig. 3 MR image of one of the patients from the control group

To evaluate the ventricular size in both groups, we measured the bifrontal and occipital horn ratio as described by O'Hayon et al. [5] (Fig. 2).

Statistical analysis

Results are presented as mean±SE of mean. Student's *t* test was used to compare the shunted and the control groups. Two-tailed *p* value of less than 0.05 was considered statistically significant.

Results

Pre-shunt CT scan evaluation

The pre-shunt CT scan for the study group patients did not reveal any feature of posterior cranial fossa abnormality. Specifically, all study patients had normal posterior fossa bony morphology without evidence of basilar invagination or superior cupping of the opisthion, no features of posterior cranial fossa neural tissue crowding, and absence of inferior cerebellar tonsillar herniation or superior cerebellar herniation through the incisura. No posterior fossa abnormalities were reported in the original, as interpreted from the neuroradiologist's transcribed report or upon study review by a second independent neuroradiologist.

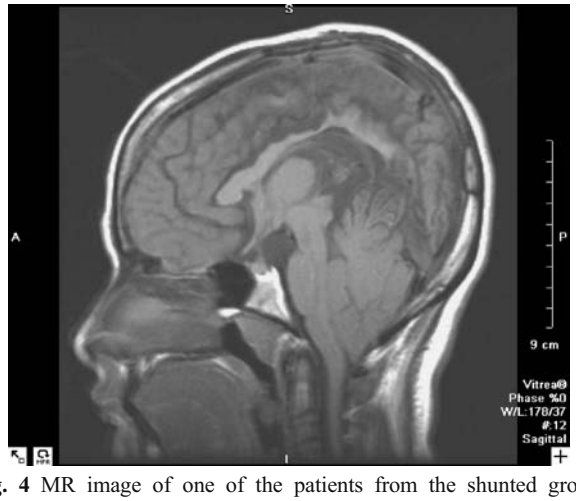

Fig. 4 MR image of one of the patients from the shunted group, showing crowding of the posterior cranial fossa contents and herniation of the cerebellar tonsils

Posterior cranial fossa volume, supratentorial volume, and cerebellar volume

Three-dimensional volumetric analysis of the MRIs demonstrated that the shunted group patients had a smaller posterior cranial fossa volume (137.9±8.5 ml) when compared to their control group peers (167.3±5.2 ml; $p<0.05$).

The supratentorial volume was greater in the shunted group (1,058.7±50.6) compared to the control group (924±52.5), although nonsignificant ($p>0.05$).

Cerebellar volume in the shunted group patients (114.1±8.8 ml) did not differ significantly from the values obtained for the control subjects. (116.8±4.6 ml; $p>0.05$).

Midsagittal T1-weighted measurements of clival length and maximal craniocaudal cerebellar length in the midline

The clival length was significantly greater in the control group (33.1±1.3 mm) compared to the shunted group (26.4±2.3 mm; $p<0.05$).

The maximal midline craniocaudal cerebellar length was significantly increased in the shunted group (59.1±5.5 mm) compared to the control group (48.6±2.4 mm; $p<0.05$).

Patients within the shunted group demonstrated evidence of inferior tonsillar herniation (8.2±1.8 mm) compared to control group values of (−2.2±1.8 mm; $p<0.05$).

Patients within the shunted group had evidence of superior cerebellar herniation (14.6±4.6 mm) compared to control group values of (0±0 mm; $p<0.05$; see Figs. 3 and 4 for sample MR images).

Prepontine and premedullary cistern dimensions

The prepontine cistern anteroposterior dimension was significantly increased in the control group (7.8±0.5 mm) than in the shunted group (4.5±0.8 mm; $p<0.05$). The anteroposterior dimension of the premedullary cistern was also increased in the control group (9.9±0.6 mm) compared to the shunted group (6.3±0.8 mm; $p<0.05$).

Ratios

Frontal and occipital horn ratio

The mean bifrontal–occipital horn ratio for the shunted group was 0.39±0.02 (range 0.31–0.5), while the mean frontal–occipital horn ratio for the control group was 0.34± 0.008. (range 0.31–0.38), indicating that there was no hydrocephalus ($p>0.05$).

Posterior fossa volume ratio

The mean posterior fossa volume ratio was greater in the control group (18.5±1.3, range 15.1–26.6) than in the shunted group (13.1±0.8, range 8.9–16.2; $p<0.003$).

Intrarater reliability

A single observer measured all the parameters. The reader was blinded to the clinical information of the patients. Each measurement was repeated at least twice and the reliability was good for all the parameters evaluated. A neuroradiologist reviewed all imaging parameters to ensure that reliable anatomic boundaries were utilized in quantitation.

Discussion

Our study demonstrates that there is a volumetric disproportion between the posterior cranial fossa and the neural content in children presenting with Chiari I symptoms after a VP shunt for hydrocephalus.

Cephalocranial disproportion secondary to VP shunt has been reported before by Hoffman and Tucker [1]. They hypothesized that shunting may lead to the development of craniosynostosis, thus resulting in Chiari I symptoms. The authors suggest that the pressure changes resulting in premature sutural closure may have been secondary to a lack of an anti-siphon device leading to overdrainage in their cohort of patients.

Although Hoffman and Tucker's hypothesis of cephalocranial disproportion due to overdrainage appears logical, we are hesitant to draw this conclusion because we have previously reported that there is no significant difference in CSF overdrainage in distal slit valve compared to its anti-siphon counterparts [6], which suggests that the type of valve may not be related to this observation of post-shunting posterior fossa overcrowding. Also, the fact that the bifrontal–occipital horn ratio within both our control and study groups was within the normal range, a finding also documented by Kulkarni et al. [7], suggests that there was no evidence of the classic "slit-like" ventricle that has been reported in cases of overshunting. In addition, post-shunting CT images were reviewed in each of our nine study patients, and there was no evidence of sutural ridging or effacement to suggest the presence of craniosynostosis.

Our finding of a nonsignificant difference in the supratentorial volume of both control and shunted groups challenges the so-called "cephalocranial disproportion." At the risk of increasing a rather growing array of terminologies to explain the Chiari phenomenon, we suggest that the mechanism is mainly a "posterior cranial fossa disproportion" because the main pathology is restricted to arrested posterior cranial fossa growth with subsequent imbalance in its growth in relation to that of its neural contents. This goes along with the findings of Nishikawa et al. [8], who defined Chiari malformation as a disease of reduction in the posterior fossa volume with overcrowding of its neural contents.

Our finding of significantly smaller posterior fossa ratio volumes in the shunted group vs the control group is in agreement with previous works. This suggests that smaller ratios are observed in Chiari patients [4].

It is possible that patients who develop post-shunting Chiari anatomy may have been predisposed to such a condition due to a congenitally small posterior fossa or abnormal cerebellar volume, but we did not find this to be the case in our study, as the posterior fossa appeared normal on the pre-shunting CT images and the cerebellar volumes matched those of age-matched control cohort. Cerebellar volumes were reported to show more of sexual rather than age dimorphism [9]. However, the volumes obtained in our shunted and age-matched control patients were both similar to those in previous studies, although the midsagittal craniocaudal dimension of the cerebellum within the shunted group patients was more than the normal standardized limits of cerebellar midline dimensions for age [10]. This finding precludes the likelihood of a primary cerebellar dysplasia in our study group and further lends credence to the assertion that cerebellar herniation occurs due to a reduction in the volume of the posterior cranial fossa.

Cranial bony development after birth depends on a complex interplay of bony and neural factors, with brain development playing a key role in the subsequent growth of the cranium. Despite the fact that our patients had no signs of overdrainage, we are aware of the fact that shunting can cause an alteration in the CSF flow dynamics without causing slit ventricles. CSF flow and dynamics are crucial in controlling the development of the brain [11]; thus, we speculate that the brain growth may have been affected due to this altered CSF compliance, thus leading to the cephalocranial disproportion observed in these patients.

The symptoms of headache, which most of these patients had, may have been due to the reduction in the volume of the posterior cranial fossa leading to elevated

pressure and compression of the brainstem contents. In addition to this, there is a possibility that the relative movement of CSF from the compressed spaces within the subarachnoid space may lead to accentuation in the brain movement within the cranium due to the inadequate CSF volume to dampen this movements. The presence of the area postrema in the floor of the fourth ventricle may have accounted for the nausea and vomiting that was exhibited by our patients.

We hypothesize that the development of the posterior fossa crowding may likely be a result of a ventriculoperitoneal gradient due to the altered flow dynamics in the subarachnoid space, thus leading to a negative pressure phenomenon with impairment in the stenting of the cranial sutures that subsequently leads to posterior cranial fossa disproportion.

We are aware that we did not have pre-shunting MR images available to obtain posterior fossa volumetrics and that we were unable to accurately obtain quantitative posterior fossa measurements on the pre-shunt CT images due to differences in slice angulation and position. Despite the small sample size and the retrospective analysis utilized in this study, we believe that the preliminary findings presented here should warrant further prospective analysis of this phenomenon with a larger patient cohort, as awareness of this entity has profound clinical significance. This is because clinical deterioration may result from ensuing brainstem compression at the level of the craniovertebral junction.

This preliminary data suggests that there is imaging evidence to support the development of an anatomy compatible with Chiari I anatomy after ventriculoperitoneal shunting in neonates with hydrocephalus secondary to intraventricular hemorrhage. Awareness of this entity has profound clinical significance, and it is pertinent to advice obtaining an MR image or considering posterior fossa decompression in shunted children with elusive symptoms of shunt failure.

References

1. Hoffman HJ, Tucker WS (1976) Cephalocranial disproportion. Childs Brain 2:167–176
2. Krogness KG (1978) Posterior fossa measurements. I. The normal size of the posterior fossa. Pediatr Radiol 6(4):193–197
3. Chen YY, Lirng JF, Fuh JL, Chang FC, Cheng HC, Wang SJ (2004) Primary cough headache is associated with posterior fossa crowdedness: a morphometric MRI study. Cephalalgia 24:694–699
4. Badie B, Mendoza D, Batzdorf U (1995) Posterior fossa volume and response to suboccipital decompression in patients with Chiari 1 malformation. Neurosurgery 37:214–218
5. O'Hanyon BB, Drake JM, Ossip MG, Tuli S, Clarke M (1998) Frontal and occipital horn ratio: a linear estimate of ventricular size for multiple imaging modalities in pediatric hydrocephalus. Pediatr Neurosurg 29:245–249
6. Virella AA, Galarza M, Masterman-Smith M, Lemus R, Lazareff J (2002) Distal slit valve and clinically relevant CSF overdrainage in children with hydrocephalus. Childs Nerv Syst 18(1–2):15–18
7. Kulkarni AV, Drake JM, Armstrong DC, Dirks PB (1999) Measurement of ventricular size: reliability of the frontal and occipital horn ratio compared to subjective assessment. Pediatr Neurosurg 31:65–70
8. Nishikawa M, Sakamoto H, Hakuba A, Nakanishi N, Inoue Y (1997) Pathogenesis of Chiari malformation: a morphometric study of the posterior cranial fossa. Neurosurgery 86:40–47
9. Escalona PR, McDonald WM, Doraiswamy PM, Boyko OB, Husain MM, Figel GS, Laskowitz D, Ellinwood EH, Krishnan KR (1991) In vivo stereological assessment of human cerebellar volume: effects of gender and age. AJNR Am J Neuroradiol 12 (5):927–929
10. Kogame S, Sawa S, Inoue Y, Fukuda T, Tada T, Shakudo M, Yahata K, Shimizu H, Onayama Y (1989) MR measurements of normal brainstem cerebellum and corpus callosum in midsagittal section. Rinsho Hoshasen 34(11):1383–1387
11. Miyan JA, Nabiyouni M, Zendah M (2003) Development of the brain: a vital role for cerebrospinal fluid. Can J Physiol Pharmacol 81(1):317–328